Modeling and Simulation of Electric Power Systems as Hybrid Systems in ISMA

EVGENY A. POPOV, YURY V. SHORNIKOV
Automated Control Systems Department
Novosibirsk State Technical University
630073, 20 Prospekt K. Marksa, Novosibirsk
RUSSIA
popov.2010@corp.nstu.ru shornikov@inbox.ru

Abstract: - Studying the dynamic behavior of electric power systems is important part of a power engineer's work. Transient phenomena in electric power systems can be naturally and conveniently modelled as hybrid or event-continuous systems, which are a generalization of classical dynamical systems. The approach is illustrated by a model of a large electric power system with controllers and protective devices. An original event detection algorithm for explicit numerical methods with error and stability control is presented and used to simulate the model. The simulation results show that the approach can be successfully applied to modeling and simulation of electric power systems. The model was composed and simulated in the modeling and simulation environment ISMA.

Key-Words: - Electric Power System, DQZ Transform, Hybrid System, Hybrid System Simulation, Stability Control, Modeling and Simulation Environment

1 Transient Phenomena in Electric Power Systems

An electric power system (EPS) is a network of elements generating, transforming (transformers, voltage stabilizers, power invertors), transmitting and distributing (power transmission lines, feeders), and consuming (loads) electrical energy along with different controllers and protective devices.

Transients might occur in an EPS due to faults or during its normal functioning. The examples are a three-phase ground fault caused by a fallen tree and change of the loads as a result of, for example, a start of an asynchronous motor at a factory. In a transient state, the currents, voltages and other system characteristics change over time. States of this kind are not preferred by the users since they expect the system properties to be more constant and predictable. For example, the power line frequency in their electrical outlets should be about $60 \pm 0.01\ Hz$ [1]. Components of the second type, controllers and protective devices, are intended for preventing damage or malfunction of the electrical elements by making transients less destructive, bringing the system to a quasi-steady state.

2 Hybrid System Approach

Although electrical components are generally described by differential-algebraic systems of equations (DAEs), that is their models are continuous, elements of the second type are discrete-continuous, more precisely the corresponding DAEs' right-hand sides have discontinuities of the first kind, or even discrete. Models of this sort can be conveniently described as hybrid systems (HS) or event-continuous systems exhibiting both discrete and continuous behaviors [2, 3]. An HS is a generalization of dynamical systems and can be regarded as a sequence of classical dynamical systems (modes) activated one after another, so the final conditions of one dynamical system are the initial conditions for the next one [4].

An *HS mode* is a tuple $< j, y^j, f^j, y_0^j >$, $j \in \{1..n_m\}$, $f_j : R \times R^{n_j} \to R^{n_j}$, where $y^j(t_0) = y_0^j$ is the initial condition for the mode behavior $y^j(t) \in R^{n_j}$, and the mode function $f^j(t, y^j)$ satisfies the Lipschitz conditions for all $(t, y^j) \in R \times R^{n_j}$ [5].

A continuously differentiable function $g(t,y): R \times R^n \to R^s$, $s = 1,2,...$ is referred to as an *event function* and is associated with the predicate $pr : g(t,y) < 0$, $pr \in B = \{false, true\}$.

The event function $g^j(t, y^j)$ of a mode behaves in such a manner that the corresponding predicate $pr_j : g^j(t, y^j) < 0$ of the mode is true ($pr_j = true$)

on the half-open interval of the mode solution $[t_j^0, t_j^*) \subseteq [t_0, t_k]$.

The *event surface* of an HS mode is the boundary $G \subset R^n$ where the event function $g(t,y)=0$.

An *event* in an HS is the HS state in the time and space $(t,y) \in R^{n+1}$ when the continuously differentiable function $g(t,y): R \times R^n \to R^s$ reaches the event surface.

Let us consider an example of a hybrid system: an electric power system. It is powered by an infinite bus, that is its voltage and frequency are constant whatever load is connected to it. A transformer, followed by a power transmission line, is connected to the infinite bus. And two loads are connected to the other end of the power transmission line via circuit breakers. The one-line diagram of the system is shown in Fig. 1.

The pair of the load L_2 and circuit breaker CB_2 can be represented as the hybrid system with two modes

$$
\begin{gathered}
L2\_On' = 0, \\
L2\_On(t_0) = 1, \\
I_{L_2}(t_0) = I_{L_{20}}; \\
On: \\
\frac{dI_{L_2}}{dt} = ..., \\
I_{2-3} = I_{L_1} + I_{L_2}, \\
g_1(t,y) = -L2\_On < 0, \\
g_2(t,y) = I_{L_2} - I_{max_{CB2}} < 0; \\
Off: \\
set\ I_{L_2}(t_0) = 0, \\
set\ L2\_On = 0, \\
\frac{dI_{L_2}}{dt} = 0, \\
I_{2-3} = I_{L_1}, \\
g_3(t,y) = L2\_On - 1 < 0,
\end{gathered}
\qquad (1)
$$

where I_{L_2} is the current through Load 2 and the corresponding circuit breaker; I_{2-3} is the current through the power transmission line; I_{L_1} is the current through Load 1 and the corresponding circuit breaker; $I_{max_{CB2}}$ is the specified maximal current through the circuit breaker CB_2; $L2\_On = 1$ means that Load 2 is connected to the EPS, whereas $L2\_On = 0$ means that the load is disconnected from the system; y is the state vector.

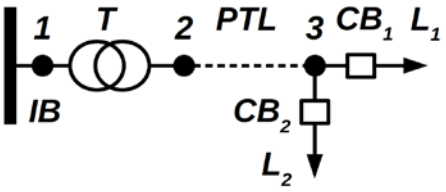

Fig. 1 Simple electric power system.

For the sake of simplicity, the rest of the model as well as the right-hand side of the differential equation for I_{L_2} are not presented.

The statechart of the system is shown in Fig. 2.

An HS mode can have one or more constraints ($s \geq 1$). In our case, the mode *On* is active as long as the circuit is not interrupted ($g_1(y,t) = -L2\_On < 0$) and the current through the circuit breaker (Load 2) is less than the specified maximum value ($g_2(y,t) = I_{L_2} - I_{max_{CB2}} < 0$). As soon as a symmetric ground fault in between L_2 and CB_2 resulting in an abnormal increase of the current through the circuit breaker occurs, the circuit breaker interrupts the circuit, so the current becomes constant and equal to zero (the *Off* mode). Then, the system can be switched on by an external command ($g_3(t,y) = L2\_On - 1 < 0$).

Let a symmetric ground fault happen at $t = 0.1s$. Fig. 3 shows plots of the currents through the loads. The circuit breaker disconnects the problematic load, which allows the system to reach a new quasi-steady state with different electrical characteristics corresponding to the change of the total load.

As events (transitions of an HS from one mode to another) may dramatically change the behavior of the hybrid system, their detection during the simulation is a crucial task. Even small errors can accumulate causing visible changes of the trajectory behavior. Failures to detect events may lead to even much worse simulation results having nothing to do with the simulated model.

3 Modeling Transients in Electric Power Systems

Let us consider another electric power system, a six-machine test system of Institute “Energosetproekt” (Russia) [6]. The one line diagram of the system is shown in Figure 4.

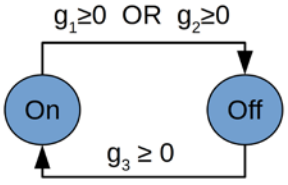

Fig. 2 Statechart.

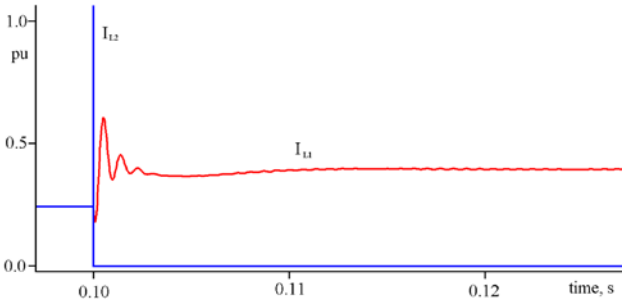

Fig. 3 Courses of I_{L_1} (red) and I_{L_2} (blue).

The system consists of six synchronous generators (G_1 – G_6), six generator transformers (T_1 – T_6 respectively), three autotransformers (AT_1 – AT_3), four loads modeling the power consumers, five power transmission lines denoted by bold dashed lines, and a current limiting reactor (R). Contrary to [6], the loads are connected to the system via circuit breakers.

The voltage rating of the power transmission lines $PTL_{7\text{-}8}$, $PTL_{8\text{-}9}$, and $PTL_{8\text{-}13}$ is 220 kV, whereas that of $PTL_{10\text{-}11}$ and $PTL_{11\text{-}12}$ is 500 kV. G_1 models a powerful hydroelectric power station (HEPS). The couples G_2, G_3 and G_4, G_5 represent a small and a large thermal power stations (TPS) respectively. The generator G_6 models the synchronous compensators (SC) installed at a transmission substation.

After applying the Park transform [7], in the corresponding rotating reference frame , generators without damper windings are described as

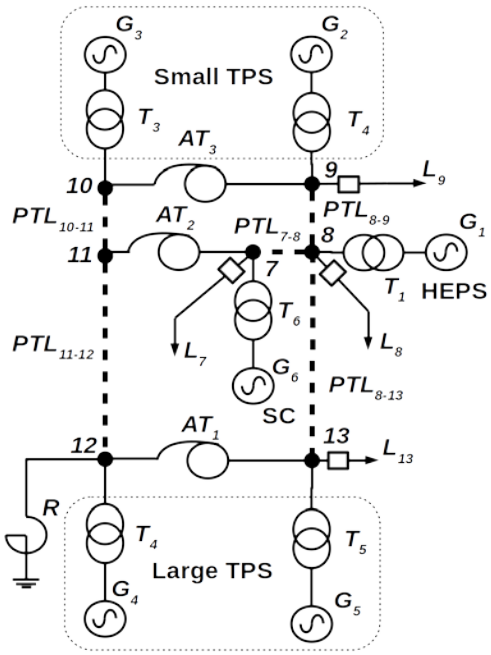

Fig. 4 One-line diagram.

$$
\begin{aligned}
\frac{d\psi_d}{dt} &= -u_d - \omega\psi_q - r_a i_d,\\
\frac{d\psi_q}{dt} &= -u_q + \omega\psi_d - r_a i_q,\\
\frac{d\psi_f}{dt} &= E_{qe}\frac{r_f}{x_{ad}} - r_f i_f,\\
\psi_d &= \frac{1}{\omega_0}(x_d i_d + x_{ad} i_f),\\
\psi_q &= \frac{1}{\omega_0} x_q i_q,\\
\psi_f &= \frac{1}{\omega_0}(x_f i_f + x_{ad} i_d),\\
\frac{d\omega}{dt} &= \frac{1}{T_J}(M_T - M),\\
M &= i_q\psi_d - i_d\psi_q,
\end{aligned}
\qquad (2)
$$

where ψ_d, ψ_q are the projections of the flux linkages of the stator windings on the axes d and q respectively; r_a is the resistance of the stator windings; u_d, u_q and i_d, i_q stand for the stator winding voltage and current projections respectively; ω denotes the angular speed of the rotor; ω_0 is the rated power line frequency; ψ_f is the flux linkage of the field winding; E_{qe} is the induced electromotive force; x_d and x_q stand for the direct and quadrature synchronous reactances respectively; x_f is the field winding reactance; r_f denotes the field winding resistance; i_f is the field winding current; x_{ad} stands for the direct stator reaction inductance; T_J is the inertia constant; M_T is the turbine torque; M is the electric torque.

All the generators are equipped with automatic voltage regulators, which stabilize the output voltages as the loads change or a fault occurs. The generators G_1 – G_5 have turbine governors.

The block diagram for the turbine governors of the generators G_2 and G_3 is shown in Fig. 5.

Given the angular speed, the controller computes the displacement of the centrifugal pendulum clutch having a dead zone [6]. The output signal, the turbine torque, is bounded to an upper limit and a lower limit by the saturation block.

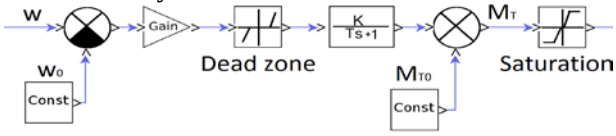

Fig. 5 Block diagram of the turbine governor.

The controller can be represented in the LISMA language [8] as shown in Fig. 6.

As long as we use Park-Gorev's equations, all the other electric equations have to be mapped onto the *d-q* frame of a reference synchronous machine [6, 7]. It results in a system of equations of coordinate transformation in the form of

$$\begin{aligned} \tilde{i}_{dj} &= i_{dj}\cos\delta_j + i_{qj}\sin\delta_j, \\ \tilde{i}_{qj} &= -i_{dj}\sin\delta_j + i_{qj}\cos\delta_j, \\ \tilde{u}_{dj} &= u_{dj}\cos\delta_j + u_{qj}\sin\delta_j, \\ \tilde{u}_{qj} &= -u_{dj}\sin\delta_j + u_{qj}\cos\delta_j, \\ \frac{d\delta_j}{dt} &= \omega_r - \omega_j. \end{aligned} \tag{3}$$

where δ_j stands for the angle between the rotors of the reference synchronous machine and synchronous machine j; $\tilde{i}_{dj}, \tilde{i}_{qj}, \tilde{u}_{dj}, \tilde{u}_{qj}$ are the projections of the current and voltage of machine j onto the axes of the reference synchronous machine. System of equations (3) is written for every synchronous machine in an EPS but the reference one.

Transformers and autotransformers can be represented as active-inductive elements as shown in Fig. 7 a. The corresponding system of equations is

$$\begin{aligned} \frac{di_d}{dt} &= \left(\frac{u_{d_i}}{x_L} - \frac{u_{d_j}}{x_L} - \frac{R}{x_L} i_d - \frac{\omega_r}{\omega_0} i_q\right)\omega_0, \\ \frac{di_q}{dt} &= \left(\frac{u_{q_i}}{x_L} - \frac{u_{q_j}}{x_L} - \frac{R}{x_L} i_q + \frac{\omega_r}{\omega_0} i_d\right)\omega_0, \end{aligned} \tag{4}$$

where $I = (i_d, i_q)^T$ is the current through the transformer or autotransformer; $U_i = (u_{d_i}, u_{q_i})^T$, $U_j = (u_{d_j}, u_{q_j})^T$ are the voltages at Nodes i and j respectively; R, x_L are the resistance and reactance.

```
1  const W0 = 1.0;
2  const SIGMA = 0.05;
3  alfa = -(w - W0) / (W0 * 3.1416 * SIGMA);
4
5  const DZ = 0.005;
6  if (abs(alfa) <= DZ) {
7     psi = 0.0;
8  }
9  else {
10    psi = (abs(alfa) - DZ) * sign(alfa);
11 }
12
13 const MT0 = 0.278880;
14 mt(t0) = MT0;
15
16 const TD = 1.0;
17 mt' = 1 / TD * (-(mt - MT0) + psi);
```

Fig. 6 Textual model of the turbine governor.

The power transmission lines are modeled as active-inductive elements with two active-capacitive connections to ground. The equivalent circuit is depicted in Fig. 7 b. The model can be simplified by neglecting the R_g components, which results in the system of equations

$$\begin{aligned} \frac{di_d}{dt} &= \left(\frac{u_{d_i}}{x_L} - \frac{u_{d_j}}{x_L} - \frac{R}{x_L} i_d - \frac{\omega_r}{\omega_0} i_q\right)\omega_0, \\ \frac{di_q}{dt} &= \left(\frac{u_{q_i}}{x_L} - \frac{u_{q_j}}{x_L} - \frac{R}{x_L} i_q + \frac{\omega_r}{\omega_0} i_d\right)\omega_0, \\ \frac{du_{d_i}}{dt} &= \left(x_C i_{d_{gi}} - \frac{\omega_r}{\omega_0} u_{q_i}\right)\omega_0, \\ \frac{du_{q_i}}{dt} &= \left(x_C i_{q_{gi}} + \frac{\omega_r}{\omega_0} u_{d_i}\right)\omega_0, \\ i_{d_i} &= i_d + i_{d_{gi}},\ i_{q_i} = i_q + i_{q_{gi}}, \\ \frac{du_{d_j}}{dt} &= \left(x_C i_{d_{gj}} - \frac{\omega_r}{\omega_0} u_{q_j}\right)\omega_0, \\ \frac{du_{q_j}}{dt} &= \left(x_C i_{q_{gj}} + \frac{\omega_r}{\omega_0} u_{d_j}\right)\omega_0, \\ i_{d_j} &= i_d - i_{d_{gj}},\ i_{q_j} = i_q - i_{q_{gj}}, \end{aligned} \tag{5}$$

where $I = (i_d, i_q)^T$ is the current through the power transmission line; $U_i = (u_{d_i}, u_{q_i})^T$, $U_j = (u_{d_j}, u_{q_j})^T$ are the voltages at Nodes i and j respectively; R, x_L are the resistance and reactance of the main branch; x_C is the reactance of the branches connected to ground; $I_i = (i_{d_i}, i_{q_i})^T$, $I_j = (i_{d_j}, i_{q_j})^T$ are the currents flowing into Node i and out of Node j respectively; $I_{gi} = (i_{d_{gi}}, i_{q_{gi}})^T$, $I_{gj} = (i_{d_{gj}}, i_{q_{gj}})^T$ are the currents through ground branches i and j respectively.

One of the simplest equivalent circuits for loads is an active-inductive element connected to ground (Fig. 8 a):

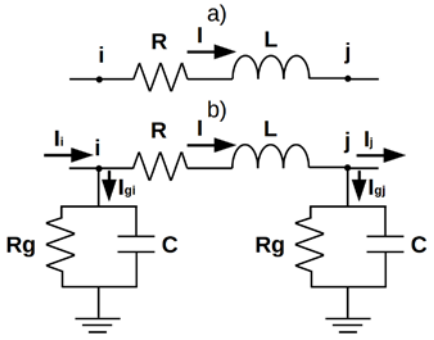

Fig. 7 Equivalent circuits for a) transformers and autotransformers, b) power transmission lines.

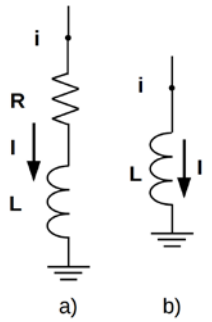

Fig. 8 Equivalent circuits for a) loads, b) reactors.

$$\frac{di_d}{dt} = \left(\frac{u_{d_i}}{x_L} - \frac{R}{x_L} i_d - \frac{\omega_r}{\omega_0} i_q\right)\omega_0,$$
$$\frac{di_q}{dt} = \left(\frac{u_{q_i}}{x_L} - \frac{R}{x_L} i_q + \frac{\omega_r}{\omega_0} i_d\right)\omega_0, \quad (6)$$

where $I = (i_d, i_q)^T$ is the current through the load; $U_i = (u_{d_i}, u_{q_i})^T$ is the voltage at Node i; R, x_L are the resistance and reactance of the load.

Reactors can be represented in the same way but with resistances of zero (Fig. 8 b), that is

$$\frac{di_d}{dt} = \left(\frac{u_{d_i}}{x_L} - \frac{\omega_r}{\omega_0} i_q\right)\omega_0,$$
$$\frac{di_q}{dt} = \left(\frac{u_{q_i}}{x_L} + \frac{\omega_r}{\omega_0} i_d\right)\omega_0, \quad (7)$$

where $I = (i_d, i_q)^T$ is the current through the reactor; $U_i = (u_{d_i}, u_{q_i})^T$ is the voltage at Node i; x_L is the reactance of the reactor.

The complete system of equations contains 144 differential and 69 algebraic equations. The given models allow one to study both electromechanical and electromagnetic transient phenomena.

4 Modeling and Simulation Environment ISMA

ISMA (the acronym for "Computer-aided analysis tools" in Russian) is a modeling and simulation environment developed by the Automated Control Systems department of Novosibirsk State Technical University (Russia) [8].

ISMA supports several input modeling languages including the textual general-purpose modeling language LISMA, a graphical language of block diagrams, and a graphical language for modeling electric power systems (Fig. 9).

ISMA's EPS editor allows one to model EPSs using the aforementioned component models, carry out simulations with different scenarios including changes of the system parameters, short circuits, line breaks.

In ISMA's EPS editor, controllers of generators as well as protective devices can be conveniently modeled using block diagrams. The model in Fig. 5 was created in ISMA's block diagram editor.

A distinctive feature of ISMA is that it allows one to use one-step explicit numerical methods with improved stability domains and stability control [9] for simulating moderately stiff [10] systems of equations, whereas it is a common practice to employ implicit methods for this purpose [11, 12].

Explicit methods, including methods with stability control, might be unacceptable to solve highly stiff problems as obtaining the solution on a transitional interval needs the step size to be very small. It may cause numerical instability as the total truncation error may exceed the desired accuracy tolerance. Moreover, such a process may take more time than when using an implicit method on this interval. From the other hand, if the stiffness is low or moderate, an explicit method with stability control might have comparable performance (in terms of the number of calculations of the right-hand side functions) to that of an implicit method on a transitional interval, as the integration step size would be chosen big enough.

The library of integration algorithms of ISMA includes original explicit multi-stage methods with improved stability domains and stability control implemented in RK2ST(2, 2), RK3ST(2, 3), DISPF(5, 6), RKF78ST(7, 13), DP78ST(8, 13), where the first number in the parentheses stands for the order of the method and the second number denotes the number of stages. The two latter algorithms are based on the Runge-Kutta-Fehlberg and Dormand-Prince schemes, whereas DISPF incorporates several explicit numerical methods of different order with stability control. The user can apply the implicit RADAU5 algorithm for solving highly stiff ODEs [5, 10]. Another original algorithm is the adaptive DISPF1_RADAU5 algorithm with stiffness detection, which combines both methods [13].

Events in HSs can be classified into three groups: unilateral, bilateral, and accuracy critical events [4]. The division is necessary because it is impossible to accurately detect a transition moment as phase space trajectories are computed using finite precision arithmetic. The problem of detection of the time instant $t = t^*$, when an event function $g(t, y(t)) = 0$, is actually a complex problem of accurate event detection [14, 15, 16].

If there are singularities or the physical meaning of a problem imposes the constraint that the phase space trajectories must not ever cross the event surface, then such cases fall into the group of unilateral events.

For event detection, ISMA employs an original event detection algorithm based on the ideas of J. Esposito [11, 14], which allows the simulator to correctly detect events. The algorithm is based on the following theorem.

Theorem. Computing the step size for an explicit numerical method of the form $y_{n+1} = y_n + h_{n+1}\varphi_n$ by using the formula

$$h_{n+1} = (\gamma - 1) g_n \left(\frac{\partial g_n}{\partial y} \varphi_n + \frac{\partial g_n}{\partial t} \right)^{-1}, \gamma \in (0,1), \quad (8)$$

guarantees the event dynamics to behave as a stable linear system approaching the surface $g(t,y) = 0$. Besides, if $g(t_0, y_0) < 0$, then $g(t_n, y_n) < 0$ for all n.

Let us consider an integration step size choice algorithm taking the event function dynamics into account for the case of a two-stage method of order two of the form

$$\begin{aligned} y_{n+1} &= y_n + p_1 k_1 + p_2 k_2, \\ k_1 &= h f(y_n),\ k_2 = h f(y_n + \beta k_1). \end{aligned} \quad (9)$$

Let the next step size with respect to the accuracy (error) and stability be computed as

$$h_{n+1}^m = max[h_n, min(h^{ac}, h^{st})], \quad (10)$$

where h_n is the latest successful integration step size, h^{ac} is the step size with respect to the accuracy (error), h^{st} is the step size with respect to stability. The next step size with respect to the accuracy h^{ac} is computed by using the formula $h^{ac} = q_1 h_n$, where q_1 is a solution to the equation $q_1^2 \| k_2 - k_1 \| = \varepsilon$.

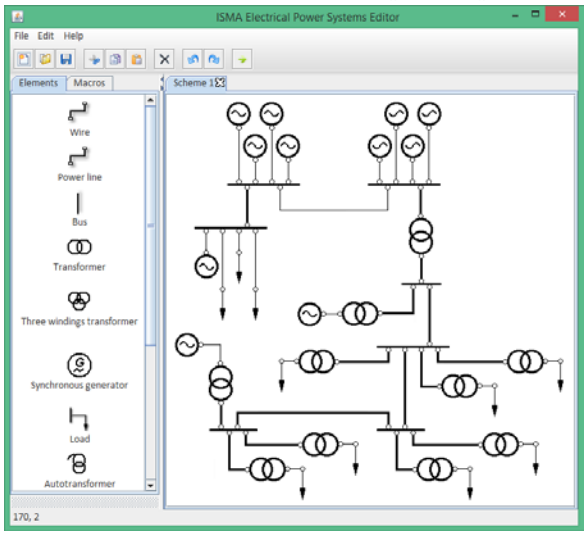

Fig. 9 ISMA's EPS editor.

The step size h^{st} with respect to stability is defined by the equation $h^{st} = q_2 h_n$, where q_2 is computed from $q_2 \upsilon_{n,2} = 2$, where $\upsilon_{n,2}$ is an estimate of the maximum Jacobian eigenvalue. Then, the following algorithm can be used to control the integration step size with respect to the accuracy (error), stability, and event function dynamics.

Step 1. Calculate $f_n = f(t_n, y_n)$.

Step 2. Calculate $g_n = g(t_n, y_n)$, $\partial g_n / \partial y = \partial g(t_n, y_n) / \partial y$, $\partial g_n / \partial t = \partial g(t_n, y_n) / \partial t$.

Step 3. Calculate $g_n' = (\partial g_n / \partial y)\varphi_n + \partial g_n / \partial t$, where the vector φ_n is equal to f_n.

Step 4. If $g_n' < 0$, then set $h_{n+1} = h_{n+1}^m$ and go to the next integration step.

Step 5. Calculate the "event step size" h_{n+1}^{ev} as $h_{n+1}^{ev} = (\gamma - 1)(g_n / g_n')$.

Step 6. Compute the step size $h_{n+1} = min(h_{n+1}^{ev}, h_{n+1}^m)$ and go to the next integration step.

In Step 4, the course of the event function is determined. If the event function approaches the event surface, the denominator of (8) is positive, and, if the event function moves away from the boundary $g(t,y) = 0$, it becomes negative. Then, once the event function course has been determined, no additional constraints on the integration step size should be imposed, if the event function moves away from the event surface.

5 Simulation

Let the load at Node 13 decrease by 10% at $t = 0s$. The reaction of the electric torque of the nearest generator G_5 is shown in Fig. 10. All the values are given in a per-unit system [7]. Apart from the electromagnetic transient, the event results in a much longer lasting electromechanical transient (Fig. 11). The oscillations decay eventually, so the system is stable in the case of such events.

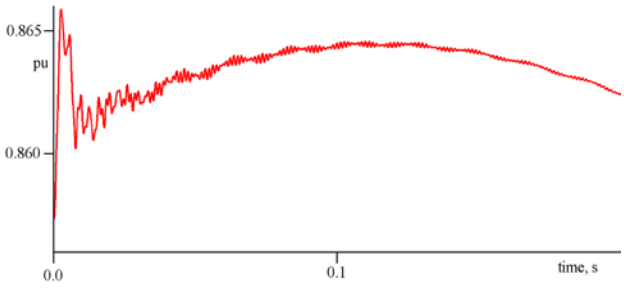

Fig. 10 Course of M_{G5}

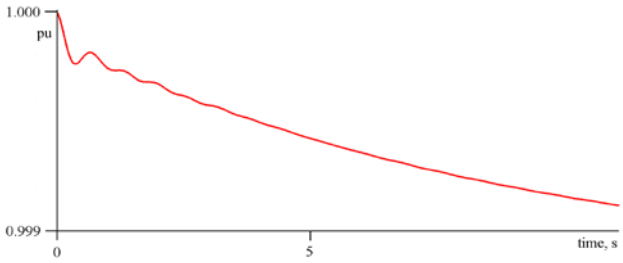

Fig. 11 Course of ω_{G5}

Now let us suppose that there happens a three-phase ground fault in between Load 9 and the corresponding circuit breaker at $t = 0.1s$. The circuit breaker interrupts the circuit almost immediately. The reaction of the electric torques of Generator 2 and Generator 4 are shown in Figures 12 and 13 respectively. The response of the farthest generator G_4 is less intensive.

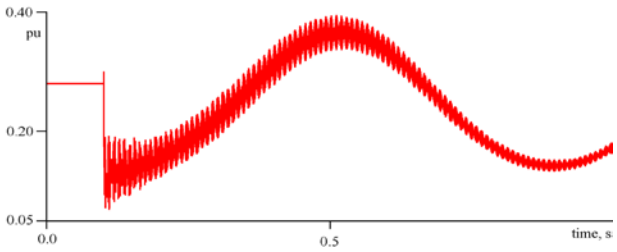

Fig. 12 Course of M_{G2}.

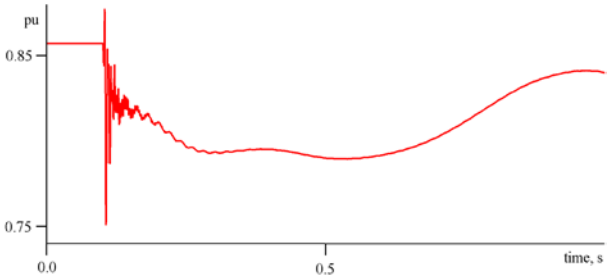

Fig. 13 Course of M_{G4}.

Figures 14, 15 show the simulations results for the case when the circuit breakers are disabled, and the same fault happens at the same place. Again, the almost self-oscillatory response of Generator 2 is more intensive than that of Generator 4, which is farther from the fault load. From the simulation results it can be concluded that the system tends to be unstable without circuit breakers in case of symmetric ground faults.

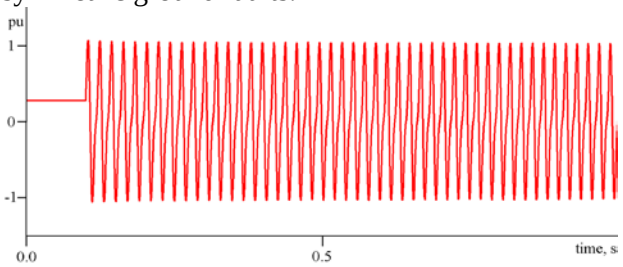

Fig. 14 Course of M_{G2} without circuit breakers

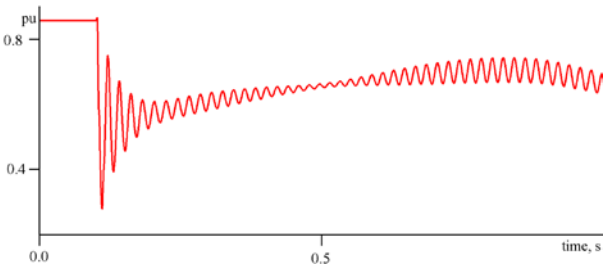

Fig. 15 Course of M_{G4} without circuit breakers

The modeling and simulation results show that hybrid system theory can be successfully applied to solving certain power engineering problems, simulating transients in electric power systems. ISMA's Electric Power System Editor facilitates the proposed techniques, including an original event detection and integration algorithms based on explicit numerical methods with improved stability domains and stability control.

Acknowledgments

This work was supported by the grant of the Russian Foundation for Basic Research (RFBR grant 17-07-01513) and by the grant of the Education, Audiovisual and Culture Agence (EU), programme ERASMUS+ Capacity building in higher education, project 573751-EPP-1-2016-1-DE-EPPKA2-CBHE-JP, Innovative teaching and learning strategies in open modelling and simulation environment for student-centered engineering education.

References:

[1] A. von Meier, *Electric Power Systems. A Conceptual Introduction*, John Wiley & Sons, 2006.

[2] P. J. Antsaklis, A Brief Introduction to the Theory and Applications of Hybrid Systems, *Proceedings of the IEEE*, Vol.88, No.7, 2000, pp.879-887.

[3] A. J. van der Schaft, H. Schumacher, *An Introduction to Hybrid Dynamical Systems*, Springer-Verlag London, 2000.

[4] J. M. Esposito, *Simulation and Control of Hybrid Systems with Applications to Mobile Robotics. Ph.D. Thesis*, University of Pennsylvania, USA, 2002.

[5] E. Hairer, S. Nørsett, G. Wanner, *Solving Ordinary Differential Equations I: Nonstiff Problems*, Springer-Verlag Berlin Heidelberg, 1993.

[6] T. Yu. Fomina, *Razrabotka algoritma raschjota pjerjehodnyh protsjessov slozhnyh rjegulirujemyh EES: dis... kand. tehn. nauk*

(Development of an Algorithm for Simulating Transients in Complex Electric Power Systems with Controllers: Candidate of Technical Sciences Thesis, Moscow Power Engineering Institute, Russia, 2014 (in Russian)

[7] V. A. Venikov, *Transient Phenomena in Electrical Power Systems*, Pergamon press, 1964.

[8] Yu. V. Shornikov, D. N. Dostovalov, Features of the ISMA Modeling and Simulation Environment, *Proceedings of the International Multi-Conference on Engineering, Computer and Information Sciences (SIBIRCON-2017)*, 2017, pp. 332-337.

[9] E. A. Novikov, M. A. Rybkov, Application of Explicit Methods with Extended Stability Regions for Solving Stiff Problems, *Mathematics & Physics*, Vol.9**,** Iss.2, 2016, pp. 209–219.

[10] E. Hairer, G. Wanner, *Solving Ordinary Differential Equations II: Stiff and Differential-Algebraic Problems*, Springer-Verlag Berlin Heidelberg, 1996.

[11] Yu. V. Shornikov, B. U. Uatay, E. A. Novikov, *Methods for Solution of Stiff Problems*, Kazakh-British Technical University Publisher, 2010.

[12] F. E. Cellier, E. Kofman, *Continuous system simulation*, Springer US, 2006.

[13] Yu. V. Shornikov, E. A. Popov, An Integration Algorithm for Simulating Stiff Electrical Networks, *Proceedings of the Moscow Workshop on Electronic and Networking Technologies (MWENT-2018)*, 2018, 5p.

[14] J. M. Esposito, V. Kumar, A State Event Detection Algorithm for Numerically Simulating Hybrid Systems with Model Singularities, *ACM Transactions on Modeling and Computer Simulation*, Vol.17, Iss.1, 2007, pp. 1-22.

[15] C. W.Gear, O. Osterby, Solving Ordinary Differential Equations with Discontinuities, *ACM transactions on mathematical software*, Vol.10**,** Iss.1, 1984, pp. 23-44.

[16] L. F. Shampine, I. Gladwell, R. W. Brankin, Reliable Solution of Special Event Location Problems for ODEs, *ACM transactions on Mathematical Software*, Vol.17, Iss.1, 1991, pp. 11–25.